

Measures to Evaluate Generative Adversarial Networks Based on Direct Analysis of Generated Images

Shuyue Guan

Department of Biomedical Engineering
The George Washington University
Washington DC, USA
frankshuyueguan@gwu.edu

Murray Loew

Department of Biomedical Engineering
The George Washington University
Washington DC, USA
loew@gwu.edu

Abstract

The Generative Adversarial Network (GAN) is a state-of-the-art technique in the field of deep learning. A number of recent papers address the theory and applications of GANs in various fields of image processing. Fewer studies, however, have directly evaluated GAN outputs. Those that have been conducted focused on using classification performance (e.g., Inception Score) and statistical metrics (e.g., Fréchet Inception Distance). Here, we consider a fundamental way to evaluate GANs by directly analyzing the images they generate, instead of using them as inputs to other classifiers. We characterize the performance of a GAN as an image generator according to three aspects: 1) Creativity: non-duplication of the real images. 2) Inheritance: generated images should have the same style, which retains key features of the real images. 3) Diversity: generated images are different from each other. A GAN should not generate a few different images repeatedly. Based on the three aspects of ideal GANs, we have designed two measures: Creativity-Inheritance-Diversity (CID) index and Likeness Score (LS) to evaluate GAN performance, and have applied them to evaluate three typical GANs. We compared our proposed measures with three commonly used GAN evaluation methods: Inception Score (IS), Fréchet Inception Distance (FID) and 1-Nearest Neighbor classifier (INNC). In addition, we discuss how these evaluations could help us deepen our understanding of GANs and improve their performance.

1. Introduction

As neural-network based generators, Generative Adversarial Networks (GANs) were introduced by Goodfellow *et al.* in 2014 [1], and they have become a state-of-the-art technique in the field of deep learning [2]. Recently, the number of types of GANs has grown to about 500 [3] and a substantial number of studies are about the theory and applications of GANs in various fields of image processing, including image translation [4], [5], object detection [6], super-resolution [7], image synthesis [8] and image blending [9]. Comparing to the theoretical progress and applications of GANs, fewer studies focus on evaluating

or measuring GANs' performance [10]. Most existing GANs' measures have been conducted using classification performance (e.g., Inception Score) and statistical metrics (e.g., Fréchet Inception Distance). Alternatively, a more fundamental approach to evaluate a GAN is to directly analyze the images it generated, instead of using them as inputs to other classifiers (e.g. Inception Network) and then analyzing the outcomes.

In this study, we try to establish fundamental ways to quantitatively and qualitatively analyze GAN-generated images. We briefly summarize three commonly used GAN evaluation methods: Inception Score (IS) [11], Fréchet Inception Distance (FID) [12], and 1-Nearest Neighbor classifier (INNC) [13], and compared those results with our two proposed measures. In addition, we discussed how these evaluations could help us to deepen our understanding of GANs and to improve their performance.

1.1. Related Work

The **Inception Score (IS)** [11] is a commonly applied index to evaluate GANs' performance. To compute the IS, we submit generated images to the Inception network [14] that was pre-trained on the ImageNet [15] dataset. From the perspective of the three aspects for ideal GANs, the IS focuses on measuring the Inheritance and Diversity. Specifically, $x \in G$ is a generated image; $y = \text{InceptionNet}(x)$ is the label obtained from the pre-trained Inception network by inputting image x . For all generated images, we have the label set Y . $H(Y)$ defines the Diversity ($H(\cdot)$ is entropy) because the variability of labels reflects the variability of images. $H(Y|G)$ could show the Inheritance because a good generated image can be well recognized and classified, and thus the entropy of $p(y|x)$ should be small. Therefore, an ideal GAN will maximize $H(Y)$ and minimize $H(Y|G)$. Equivalently, the goal is to maximize: $H(Y) - H(Y|G)$

$$\begin{aligned} &= -\sum_y p(y) \log p(y) - \sum_x p(x) H(y|x) \\ &= \sum_y p(y) \log \frac{1}{p(y)} + \sum_x \sum_y p(x) p(y|x) \log p(y|x) \end{aligned}$$

Since $\sum_x p(x) = 1$

$$= \sum_x \sum_y \left[p(x) p(y|x) \log \frac{1}{p(y)} + p(x) p(y|x) \log p(y|x) \right]$$

$$\begin{aligned}
&= \sum_x p(x) \sum_y p(y|x) \log \frac{p(y|x)}{p(y)} \\
&= \sum_x p(x) \mathbf{D}_{KL}[p(y|x)||p(y)] = \mathbf{E}_G[\mathbf{D}_{KL}(p(y|x)||p(y))]
\end{aligned}$$

\mathbf{D}_{KL} is the Kullback–Leibler (KL) divergence of two distributions [16]. The IS index is defined:

$$IS(G) = \exp(\mathbf{E}_G[\mathbf{D}_{KL}(p(y|x)||p(y))])$$

The IS reflects Inheritance and Diversity; a larger value of IS indicates that a GAN's performance is better. The limitations of IS are obvious: it **depends on classification of images by the Inception network**, which is by trained ImageNet. Thus, it may not be proper to use on other images or non-classification tasks. Also, since the Creativity is not considered by the IS, it has no ability to detect overfitting.

Fréchet Inception Distance (FID) [12] also uses the pre-trained Inception network. Instead of output labels it uses feature vectors from the final pooling layers of InceptionNet. All real and generated images are input to the network to extract their feature vectors.

Let $\varphi(\cdot) = \text{InceptionNet_lastPooling}(\cdot)$ be the feature extractor. $F_r = \varphi(R), F_g = \varphi(G)$ are two groups of feature vectors extracted from real and generated image sets. Consider the distributions of F_r, F_g are multivariate Gaussian:

$$F_r \sim N(\mu_r, \Sigma_r); F_g \sim N(\mu_g, \Sigma_g)$$

The difference of two Gaussians is measured by the Fréchet distance:

$$FID(R, G) = \|\mu_r - \mu_g\|_2^2 + \text{Tr}(\Sigma_r + \Sigma_g - 2(\Sigma_r \Sigma_g)^{1/2})$$

In fact, FID measures the difference between distributions of real and generated images; that agrees with the goal of GAN training – to minimize the difference between the two distributions. But the **Gaussian distribution assumption** of feature vectors cannot be guaranteed. And, as with IS, it depends on the pre-trained Inception network.

The measure: **1-Nearest Neighbor classifier (1NNC)** [13] does not require an additional classifier. Instead, it uses a two-sample test with the 1-Nearest Neighbor method on real and generated image sets. Similar to FID, 1NNC examines whether two distributions of real and generated image are identical, but it requires the numbers of real and generated images to be equal.

Suppose $|R| = |G|$, and we wish to compute the leave-one-out (LOO) accuracy of a 1-NN classifier trained on R and G with labels “1” for R and “0” for G . In the optimal situation, the LOO accuracy ≈ 0.5 because the two distributions are very similar. If LOO accuracy < 0.5 , the GAN is overfitting to R because the generated data are very close to the real samples. In an extreme case, if the GAN memorizes every sample in R and then generates them identically, i.e., $G = R$, the accuracy would be 0 because every sample from R would have its nearest neighbor from G with zero distance. LOO accuracy > 0.5 means the two distributions are different (separable). If they are completely separable, the accuracy would be 1.0.

Compared to IS and FID, 1NNC seems a more independent measure. However, the $|R| = |G|$ requirement limits its applications and **the local conditions of distributions** will greatly affect the 1-NN classifier. For IS, higher values imply better performance of GANs; and for FID, lower is better. But for 1NNC, 0.5 is the best score. We regularize 1NNC by this function:

$$r(x) = -|2x - 1| + 1$$

$r1NNC = r(1NNC)$. For r1NNC, the best score is 1.

1.2. GAN Evaluation Metrics

The optimal GAN for images can generate images that have the same distribution as real samples (used for training), are different from real ones (not duplication), and have variety. Expectations of generated images could be described by three aspects: 1) non-duplication of the real images, 2) generated images should have the same style, which means their distribution is close to that of the real images, and 3) generated images are different from each other. Therefore, we evaluate the performance of a GAN as an image generator according to **the three aspects**:

- Creativity**: non-duplication of the real images. It checks for overfitting by GANs.
- Inheritance**: generated images should have the same style, which retains key features of the real (input) images. And this is traded off with the creativity property because generated images should not be too similar nor too dissimilar to the real ones.
- Diversity**: generated images are different from each other. A GAN should not generate a few dissimilar images repeatedly.

Fig. 1 displays four counterexamples of ideal generated images.

First, we have designed three measures to evaluate GAN performance according to the three expectations of ideal generated images. These measures applied indexes for digital image analysis to measure difference or similarity between images, such as image moment, gray-level co-occurrence matrix (GLCM), and structural similarity (SSIM) [17] index. Then, the **CID index** is defined by multiplication of the three proposed measures.

Second, inspired by SSIM, we constructed a more direct way to measure difference or similarity between images based on the Euclidean distance. We introduced a distance-based separability index and used it to define another measure: Likeness Score (LS) for GAN evaluations. Compared to the CID index, LS has a simpler and more uniform framework for the three aspects of ideal GANs and depends less on visual evaluation.

The proposed two measures are applied to analyze the generated images directly, without using pre-trained classifiers. We applied the measures to outcomes of three

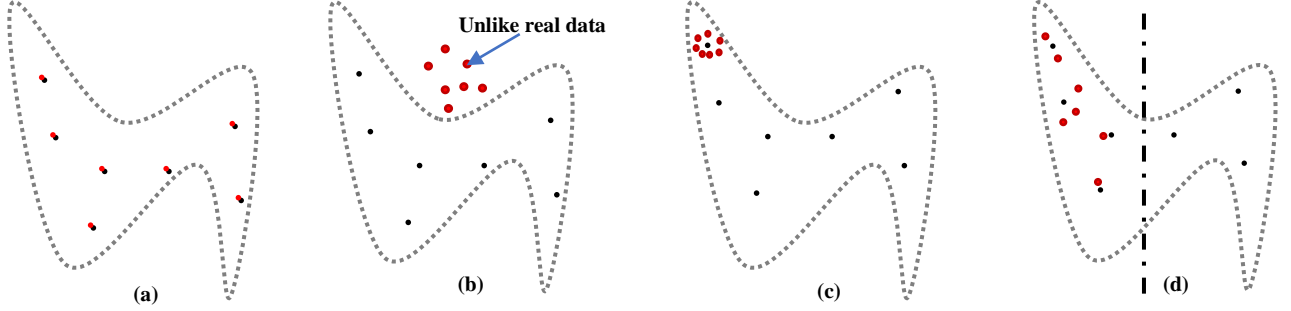


Fig. 1 Problems of generated images in perspective of distribution. The area of dotted line is the distribution of real images. The dark-blue dots are real samples and red dots are generated images. (a) is overfitting, lack of Creativity. (b) is lack of Inheritance. (c) is called mode collapse for GAN and (d) is mode dropping. Both (c) and (d) are lack of Diversity.

typical GANs: DCGAN [18], WGAN-GP [19] and SNGAN [20]. Results show that our proposed measures do reflect the performance of GAN well and are very competitive with other compared measures. In addition, they are stable with respect to the number of images and could provide explanation of results in terms of the three respects of ideal GANs.

2.Creativity-Inheritance-Diversity index

Consider a set of real images: $R = \{I_r\}$. A GAN has been trained by this real image set and a set of synthetic images were generated from the GAN: $G = \{I_g\}$.

The **Creativity** measure is to find duplications of real images. To I_g , the duplication occurs when the SSIM between I_g and any I_r is equal to or greater than 0.8¹.

Algorithm 1 Creativity measure

```

1: Input real images:  $R = \{I_r\}$  and generated images:
    $G = \{I_g\}$ .
2:  $G^{rem} \leftarrow G$ 
3: for  $I_g$  in  $G^{rem}$  do
4:   for  $I_r$  in  $R$  do
5:     if  $SSIM(I_g, I_r) \geq 0.8$  then
6:       remove  $I_g$  from  $G^{rem}$ 
7:     break
8:   end if
9:   end for
10: end for
11: return  $|G^{rem}|/|G|$ 

```

After removing duplications of real samples from G , G^{rem} is the set of remaining generated images. Creativity index is the percentage of remaining images.

The main idea to measure **Inheritance** is that same-type images have similar textures. We applied the GLCM-contrast to all real and generated images and Inheritance index is the difference between average GLCM-contrast value of set R and G^{rem} .

Algorithm 2 Inheritance measure

```

1: Input images:  $R$  and  $G^{rem}$ .
2:  $gc_r \leftarrow$  average GLCM-contrast of  $R$ 
3:  $gc_g \leftarrow$  average GLCM-contrast of  $G^{rem}$ 
4: return  $1 - |gc_r - gc_g|/\max\{gc_r, gc_g\}$ 

```

To compute the **Diversity** index, SSIM is used again to group similar generated images to the same cluster. Then, we calculate the entropy of these clusters. More clusters and fewer images in each cluster indicate that generated images are more diverse. The optimal condition is that every cluster has only one image; in this case, the entropy value is maximum.

Algorithm 3 Diversity measure

```

1: Input  $G^{rem}$ ;  $i \leftarrow 1$ 
2: repeat
3:   select one image  $I_g \in G^{rem}$  and move to  $C_i$ 
4:   for  $I$  in  $G^{rem}$  do
5:     if  $SSIM(I_g, I) \geq 0.8$  then
6:       move  $I$  from  $G^{rem}$  to  $C_i$ 
7:     end if
8:   end for
9:    $i \leftarrow i + 1$ 
10: until  $G^{rem} = \emptyset$ ; to have  $m$  clusters:  $C_1 \dots C_m$ 
11: return  $-\sum_i^m p_i \log p_i$ ;  $p_i \leftarrow |C_i|/\sum_i^m |C_i|$ 

```

The product of the three measures is the comprehensive measure (CID index):

$$CID = Creativity \times Inheritance \times Diversity$$

3.Likeness Score

Because the FID and INNC are effective ways to examine how the distributions of real and generated images are close to each other, they are also an effective way to measure GANs because the goal of GAN training is to make generated images have the same distribution as real ones. Consider a two-class dataset in which real data and

¹ See Sec.5 for a discussion of this value.

generated data sets are defined by the maximum entropy principle (MEP); this is the most difficult situation for separation of the data because the two classes of data are **scattered and mixed together in the same distribution**. In this sense, the **separability** of real and generated data could be a promising measure of the similarity of the two distributions. As the separability increases, the two distributions have more differences.

Based on MEP, we could define the data separability as being inversely related to the system's entropy. To calculate the entropy, we divide the space into many small regions. Then, the proportions of each class in every small region can be considered as their occurrence probabilities. The system's entropy can be derived from those probabilities. In high-dimensional spaces for images, however, the number of small regions grows exponentially. For example, for 32x32 pixels 8-bit RGB images, the space has 3,072 dimensions. If each dimension (the range is from 0 to 255) is divided to 32 intervals, the total number of small regions is $32^{3072} \approx 6.62 \times 10^{4623}$. It is impossible to compute the system's entropy in this way.

Alternatively, we propose the **Distance-based Separability Index (DSI)** as a substitute of entropy to analyze how the two classes of data are mixed together. Consider two classes X, Y that have the same distribution covering the same region and have sufficient points. Suppose X, Y have N_x, N_y points, we define that the **Intra-Class distance (ICD) set** is the set of distances between any two points in the same class (X):

$$\{d_x\} = \left\{ \|x_i - x_j\|_2 \mid x_i, x_j \in X; x_i \neq x_j \right\}$$

If $|X| = N_x$, then $|\{d_x\}| = \frac{1}{2} N_x(N_x - 1)$.

And the **Between-class distance (BCD) set** is the set of distances between any two points from different classes (X, Y):

$$\{d_{x,y}\} = \left\{ \|x_i - y_j\|_2 \mid x_i \in X; y_j \in Y \right\}$$

If $|X| = N_x, |Y| = N_y$, then $|\{d_{x,y}\}| = N_x N_y$.

It can be proven¹ that: if and only if two classes X, Y have the same distribution covering the same region and have sufficient points, the distributions of ICD and BCD sets are nearly identical. Hence, if the distributions of the ICD and BCD sets are nearly identical, the system has the maximum entropy and thus has the worst separability. The metric of distance is Euclidean (l^2 -norm). The time cost for ICD and BCD sets is linear growth to dimension and quadratic growth to the number of observations. It is much better than computing the system's entropy by dividing the space into many small regions.

¹ We do not show the proof here because it is detailed and not relevant to the main topic. It will appear in another forthcoming publication. Since the statement is intuitive, we provide an informal explanation here: points in X, Y having the same distribution and covering the same region can be considered to have been sampled from one distribution Z. Hence, both ICDs of X, Y and BCDs between X, Y are **actually ICDs of Z**. Consequently, the distributions of ICDs and BCDs are identical.

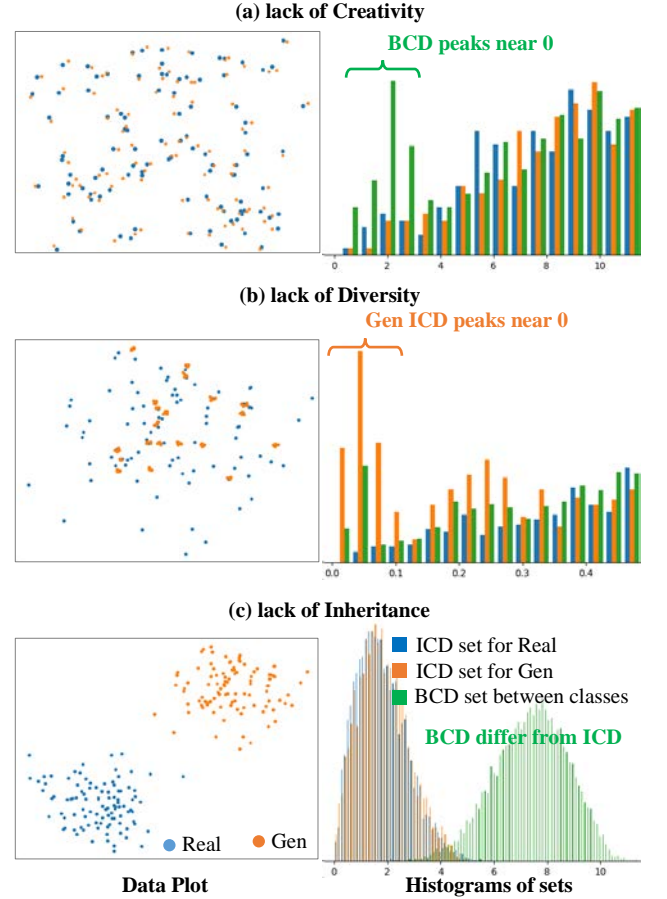


Fig. 2. Lack of Creativity, Diversity and Inheritance in 2D. Histograms of (a) and (b) are zoomed to ranges near zero; (c) has the entire histogram.

3.1. Computation of DSI

First, we compute the ICD sets of real image set R and generated image set G : $\{d_r\}, \{d_g\}$ and the BCD set: $\{d_{r,g}\}$. To examine the similarity of the distributions of ICD and BCD sets, we apply the Kolmogorov–Smirnov test (KS-test) [21]. Although there are many statistical measures to compare two distributions, such as Bhattacharyya distance, Kullback–Leibler divergence and Jensen–Shannon divergence, most of them require that the two sets have the same number of observations. It is easy to show that the $|\{d_r\}|, |\{d_g\}|$ and $|\{d_{r,g}\}|$ cannot be the same length. Then, to compute the similarities between ICD sets and BCD sets by the KS-test: $s_r = KS(\{d_r\}, \{d_{r,g}\})$, $s_g = KS(\{d_g\}, \{d_{r,g}\})$. The DSI is the maximum of two KS similarities: $DSI(\{R, G\}) = \max\{s_r, s_g\}$ because the

maximum value can highlight the difference between ICD and BCD sets. $KS(\{d_r\}, \{d_g\})$ is not considered because it shows only the difference of distribution shapes, not including their location information. For example, two distributions that have the same shape, but no overlap will have similarities between ICD: $KS(\{d_1\}, \{d_2\})$ equal to zero.

3.2. DSI and GAN Evaluation

Algorithm 4 Likeness Score

```

1: Input real images:  $R = \{I_r\}$  and generated images:
    $G = \{I_g\}$ .
2:  $\{d_r\} = \{d_g\} = \{d_{r,g}\} = \emptyset$ 
3: for  $I_r$  in  $R$  do
4:   for  $I'_r$  in  $R$  and  $I'_r \neq I_r$  do
5:      $\{d_r\} = \{d_r\} + \{\|I'_r - I_r\|_2\}$ 
6:   end for
7: end for
8: for  $I_g$  in  $G$  do
9:   for  $I'_g$  in  $G$  and  $I'_g \neq I_g$  do
10:     $\{d_g\} = \{d_g\} + \{\|I'_g - I_g\|_2\}$ 
11:   end for
12: end for
13: for  $I_r$  in  $R$  do
14:   for  $I_g$  in  $G$  do
15:      $\{d_{r,g}\} = \{d_{r,g}\} + \{\|I_r - I_g\|_2\}$ 
16:   end for
17: end for
17:  $s_r = KS(\{d_r\}, \{d_{r,g}\})$ ,  $s_g = KS(\{d_g\}, \{d_{r,g}\})$ 
18: return  $1 - \max\{s_r, s_g\}$ 

```

Fig. 2 displays examples of situations in 2D that generated data that lack Creativity, Diversity, and Inheritance. With respect of ICD and BCD sets, if the generated data overfit the real data (lack of Creativity), peaks will appear in the distribution of BCD near zero (see Fig. 2a) because there are many generated points that are close to real data points in their distribution space; hence, many BCD are close to zero. Similarly, lack of Diversity implies that many generated data points are close to each other; thus many ICD are close to zero and peaks will appear in the distribution of ICD near zero (see Fig. 2b). Lack of Inheritance is shown by the difference between the distribution of ICD and BCD (see Fig. 2c) because if and only if two classes (real data and generated data) have the same distribution (shapes) covering the same region, the distributions of ICD and BCD sets are identical. In fact, if the distributions of the ICD and BCD sets are identical, there is neither lack of Creativity nor lack of Diversity. This is because there will be **no single peaks of ICD or BCD near zero**. Therefore, the DSI could evaluate the GAN’s performance well. DSI ranges from 0 to 1; DSI is close to 1 when the distributions of real and generated data are more different. To be consistent with

other comparison measures, we complement its value and define the **Likeness Score (LS)** $= 1 - DSI$, which is closer to 1 if the GAN performs better.

4. Experiments & Results

The first experiment is to test the stability of measures to different numbers of data. One purpose is to ensure our proposed measures are not changed by different numbers of data. Another purpose is to find a proper number of data for next experiment because GAN could generate infinite data and too many data make computing slow. The second experiment is to compare our new measures with some commonly used measures. The purpose is not to show which GAN is better but to show how the results (values) of our measures match with compared measures.

4.1. One image type by DCGAN

Table 1. Measure values for different numbers of generated images

#	C	I	D	CID	LS	IS	FID	r1NNC
120	0.083	0.965	1.748	0.141	0.613	1.435	148.527	0.808
240	0.079	0.938	2.288	0.170	0.644	1.424	134.484	0.696
480	0.106	0.956	2.602	0.264	0.636	1.409	135.317	0.738
960	0.083	0.946	2.650	0.209	0.622	1.447	145.142	0.748
1200	0.086	0.947	2.441	0.199	0.630	1.426	141.818	0.727
2400	0.095	0.953	2.749	0.249	0.628	1.431	146.109	0.734
4800	0.094	0.937	2.714	0.238	0.622	1.440	145.109	0.758

* Dotted line: to the left are our proposed measures; to the right are compared measures.

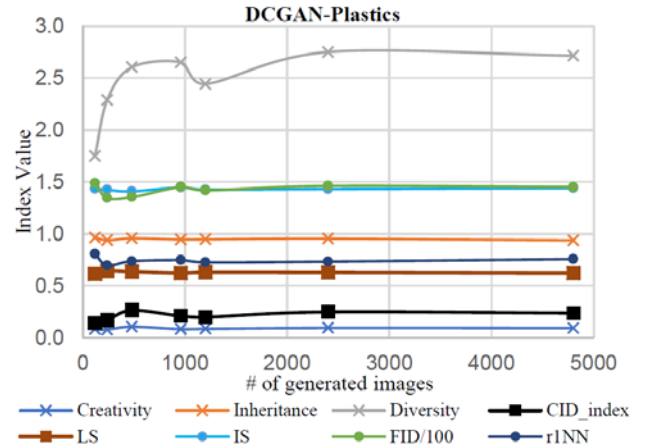


Fig. 3 Plots of values in Table 1.

To test the proposed measures, in the first experiment, we used one type of image (Plastics; 12 images) from the USPTex database [22] to train a DCGAN. Then, the trained GAN generated several groups containing different numbers of synthetic images. Finally, we compute our proposed measures, IS, FID and r1NNC results by using these

generated images and 12 real images; the results are shown in Table 1.

Computations of **FID and r1NNC require that the two image sets have same number of images**. We divided the generated images into many 12-image subsets to compute the indexes with 12 real images and then found their average values. Fig. 3 shows the plots of these indexes. FID is scaled by 0.01 to fit the axes. The result indicates that these indexes are stable to different numbers of testing images, especially when the number is greater than 1000.

4.2. Four image types and three GANs

In the second experiment, four types of image (Holes, Small leaves, Big leaves and Plastics; 12 images for each type) are used to train three GANs (DCGAN, WGAN-GP and SNGAN). Then, the trained GANs generated 1,200 synthetic images for each type. Twelve sets of synthetic images were generated; Fig. 4 shows samples from 4 real image sets and 12 generated image sets. Visual examination of these synthetic images indicates that the DCGAN seems to give the most images similar to the real ones, but many of its generated images are duplications of real ones. Thus, the DCGAN overfitted the training data. The SNGAN's generated images are most dissimilar to real images; it lacks Inheritance feature. The WGAN-GP well balanced the Creativity and Inheritance features.

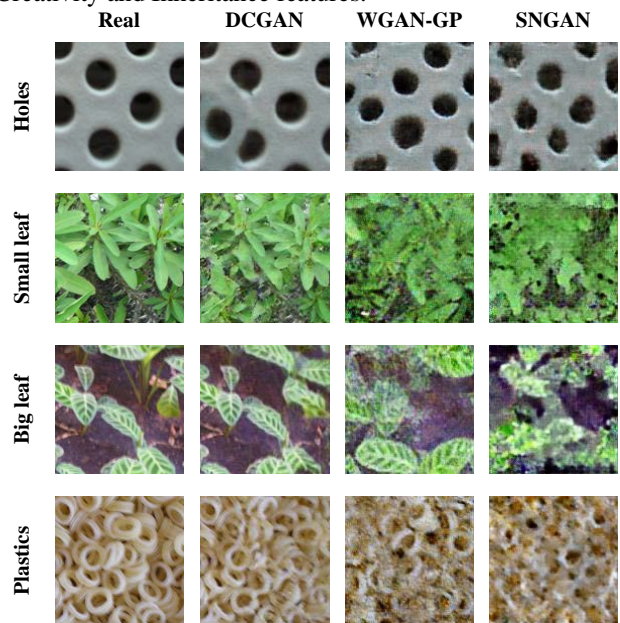


Fig. 4 Column 1: samples from 4 types' real image; column 2-4: samples from synthetic images of 3 GANs trained by the 4 types' images

Finally, we applied these measures on the 12 generated image sets; results are shown in Table 2. Fig. 5 shows plots of results. To emphasize the order of each index for different

generators and image type, values are normalized from 0 to 1 by columns for plotting. Table 3 averaged scores by GANs.

To compare the three GANs, Table 3 shows summarized results and Fig. 5 gives more details. For the best generator, the proposed CID index and LS agrees with IS, 1NNC and looks of generated images. Since DCGAN overfitted to training data, its Creativity score is the lowest, but FID thinks it is the best model and FID thinks SNGAN is the worst because its Diversity index is the lowest. At this point, FID agrees with LS, IS and 1NNC.

Table 2. Measure results

*	C	I	D	CID	LS	IS	FID	r1NNC
DC-hol	0.153	0.768	4.495	0.527	0.747	1.222	102.805	0.763
DC-sl	0.209	0.863	2.085	0.376	0.611	1.171	155.973	0.504
DC-bl	0.091	0.899	2.658	0.217	0.262	1.321	172.296	0.218
DC-pla	0.086	0.947	2.441	0.199	0.630	1.426	141.818	0.727
W-hol	1.000	0.800	5.816	4.655	0.771	1.163	233.277	0.721
W-sl	1.000	0.927	6.437	5.965	0.465	1.369	400.036	0.947
W-bl	1.000	0.754	6.953	5.243	0.626	1.536	375.987	0.980
W-pla	1.000	0.799	6.888	5.502	0.441	1.555	513.268	0.942
SN-hol	0.977	0.970	3.584	3.393	0.594	1.317	252.857	0.592
SN-sl	1.000	0.975	0.527	0.514	0.025	1.105	469.795	0.477
SN-bl	1.000	0.726	0.088	0.064	0.000	1.083	456.813	0.000
SN-pla	1.000	0.792	0.000	0.000	0.000	1.037	485.716	0.001

* Generator models: DC: DCGAN; W: WGAN-GP; SN: SNGAN. Generated image types: hol: holes; sl: small leaves; bl: big leaves; pla: plastics. Dotted line: to the left are our proposed measures; to the right are the compared measures.

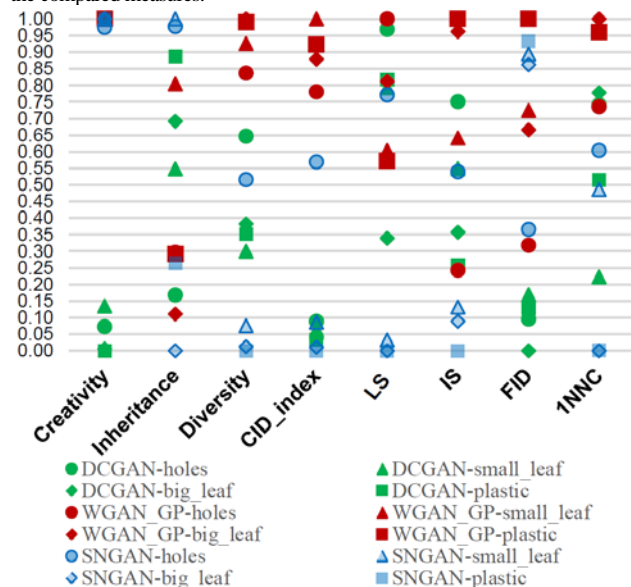


Fig. 5 Normalized indexes. X-axis shows indexes and y-axis shows their normalized values. Colors are for generators and shapes are for image types; see details in legend.

Table 3. Measure results averaged by generators

*	C	I	D	CID	LS	IS	FID [†]	r1NNC
DC	<u>0.135</u>	0.869	2.920	<u>0.330</u>	0.562	1.285	<u>143.223</u>	0.553
W	1.000	<u>0.820</u>	6.524	5.341	0.576	1.406	380.642	0.897
SN	0.994	0.866	<u>1.050</u>	0.993	<u>0.155</u>	<u>1.135</u>	416.295	<u>0.267</u>

* Generator models: DC: DCGAN; W: WGAN-GP; SN: SNGAN. **Bold**: the highest score in column. Underline: the lowest score in column. Dotted line: to the left are our proposed measures; to the right are the compared measures. [†] FID: lower is better.

5. Discussion

The results in Table 3 indicate that our proposed measures, CID index and LS, better reflects the GANs’ performances when evaluated visually, and the performance rank of LS agrees with IS and 1NNC. Although DCGAN has the highest Inheritance feature, most of its synthetic images are duplications of real ones. Since overfitting is a serious problem for GANs, DCGAN does not obtain the best score for integrated measures except FID. CID penalizes the lack of Creativity more. SNGAN and WGAN-GP generate synthetic images that look different from real samples; thus, their Creativity scores are high. SNGAN, however, tends to generate very similar images; its Diversity score is low. Hence, LS, IS, FID and 1NNC think SNGAN performing worst because these measures may emphasize the generator’s Diversity feature more. Compared with LS, IS, FID and 1NNC, the CID considers the Creativity feature (overfitting) to be a more important factor. WGAN-GP has the best scores for Creativity and Diversity features while maintaining a good Inheritance feature (close to DCGAN). Therefore, it obtains the highest CID, LS, IS, and 1NNC scores.

To measure the Inheritance, we used GLCM-contrast. The GLCM works for texture analysis but may not be the best analysis method for non-texture images. In this study, we selected four texture images. (Other measures exist for non-textural images.) And, to measure the Creativity and Diversity, the threshold for SSIM is 0.8. This threshold will greatly influence the results and requires further study. In addition, the SSIM is used to evaluate the Creativity of GANs after training. We note that H. Zhao et al. (2017) [23] introduced the Multi-Scale Structural Similarity (MS-SSIM) loss for training GANs. If we apply the MS-SSIM loss to train GANs, the Creativity feature could be directly improved.

Both CID and LS use image comparisons. CID uses the SSIM and LS uses the Euclidean (l^2 -norm) distance. In the worst case, their time complexities are $O(N^2)$, where N is the total number of compared images. But for one comparison, the Euclidean distance is computed (9.37×10^{-5} s) about 167 times faster than SSIM (1.56×10^{-2} s) in our computer. As Table 4 shown, in one experiment, LS is computed faster than CID.

Table 4. Time cost of measures

Measure	CID	LS	IS	FID	r1NNC
Time (s)	45.183	25.608	8.928	24.677*	0.275*

* Time costs of FID and r1NNC are for 12 real vs. 12 generated images because FID and r1NNC require two image sets that have the same number of images. CID, LS, and IS used 12 real vs. 1,200 generated images.

The CID index is designed directly from the three aspects of ideal GANs. However, it measures the three aspects by different techniques. Those techniques have many limitations in their application to various types of images, and the results highly depend on the selected threshold. In contrast, LS solved these problems. Although LS uses a very simple process -- it does not need any pre-trained classifier, image analysis methods, nor *a priori* knowledge of distributions -- it has been proved effective. LS calculates only Euclidean distances and then applies the KS-test; those methods are independent of image types, numbers, and sizes. We have shown that LS also considers the three aspects of ideal GANs in a uniform framework. In general, LS is more like 1NNC but LS does not require $|R|=|G|$ and is not affected by local conditions of the distributions.

Results also show that a GAN that performs well with one type image may not be do so with other types. For example, from Table 2 and Fig. 5, we see that when measured by CID, LS, IS, FID and 1NNC, the SNGAN performs much better on Holes images than on other types. Hence, in future works, we will examine the proposed measures on more types of images and GAN models.

6. Conclusion

Our proposed measures, the CID index and LS, can directly analyze the generated images without using a pre-trained classifier and they are stable with respect to the number of images. Hence, they have fewer constraints and wider applications than some existing GAN measures, such as IS, FID, and 1NNC. Furthermore, they could evaluate the performance of GANs well and provide explanation of results in the three main respects of optimal GANs according to our predictions of ideal generated images. Such explanations help us to deepen our understanding of GANs and of other GAN measures that will help to improve GANs performance.

References

- [1] I. Goodfellow *et al.*, “Generative Adversarial Nets,” in *Advances in Neural Information Processing Systems 27*, Z. Ghahramani, M. Welling, C. Cortes, N. D. Lawrence, and K. Q. Weinberger, Eds. Curran Associates, Inc., 2014, pp. 2672–2680.
- [2] Y. Hong, U. Hwang, J. Yoo, and S. Yoon, “How Generative Adversarial Networks and Their Variants Work: An Overview,” *ACM Comput. Surv.*, vol. 52, no. 1, pp. 1–43, Feb. 2019.
- [3] A. Hindupur, *the-gan-zoo: A list of all named GANs!* 2018.
- [4] C. Wang, C. Xu, C. Wang, and D. Tao, “Perceptual Adversarial Networks for Image-to-Image Transformation,” *IEEE Trans. Image Process.*, vol. 27, no. 8, pp. 4066–4079, Aug. 2018.
- [5] Z. Yi, H. Zhang, P. Tan, and M. Gong, “DualGAN: Unsupervised Dual Learning for Image-to-Image Translation,” in *2017 IEEE International Conference on Computer Vision (ICCV)*, Venice, 2017, pp. 2868–2876.
- [6] J. Li, X. Liang, Y. Wei, T. Xu, J. Feng, and S. Yan, “Perceptual Generative Adversarial Networks for Small Object Detection,” in *2017 IEEE Conference on Computer Vision and Pattern Recognition (CVPR)*, Honolulu, HI, 2017, pp. 1951–1959.
- [7] C. Ledig *et al.*, “Photo-Realistic Single Image Super-Resolution Using a Generative Adversarial Network,” in *2017 IEEE Conference on Computer Vision and Pattern Recognition (CVPR)*, Honolulu, HI, 2017, pp. 105–114.
- [8] Z. Pan, W. Yu, X. Yi, A. Khan, F. Yuan, and Y. Zheng, “Recent Progress on Generative Adversarial Networks (GANs): A Survey,” *IEEE Access*, vol. 7, pp. 36322–36333, 2019.
- [9] H. Wu, S. Zheng, J. Zhang, and K. Huang, “GP-GAN: Towards Realistic High-Resolution Image Blending,” in *Proceedings of the 27th ACM International Conference on Multimedia - MM '19*, Nice, France, 2019, pp. 2487–2495.
- [10] A. Borji, “Pros and cons of GAN evaluation measures,” *Comput. Vis. Image Underst.*, vol. 179, pp. 41–65, Feb. 2019.
- [11] T. Salimans *et al.*, “Improved Techniques for Training GANs,” in *Advances in Neural Information Processing Systems 29*, D. D. Lee, M. Sugiyama, U. V. Luxburg, I. Guyon, and R. Garnett, Eds. Curran Associates, Inc., 2016, pp. 2234–2242.
- [12] M. Heusel, H. Ramsauer, T. Unterthiner, B. Nessler, and S. Hochreiter, “GANs Trained by a Two Time-Scale Update Rule Converge to a Local Nash Equilibrium,” in *Advances in Neural Information Processing Systems 30*, I. Guyon, U. V. Luxburg, S. Bengio, H. Wallach, R. Fergus, S. Vishwanathan, and R. Garnett, Eds. Curran Associates, Inc., 2017, pp. 6626–6637.
- [13] D. Lopez-Paz and M. Oquab, “Revisiting Classifier Two-Sample Tests,” in *International Conference on Learning Representations*, 2017.
- [14] C. Szegedy, V. Vanhoucke, S. Ioffe, J. Shlens, and Z. Wojna, “Rethinking the Inception Architecture for Computer Vision,” in *2016 IEEE Conference on Computer Vision and Pattern Recognition (CVPR)*, Las Vegas, NV, USA, 2016, pp. 2818–2826.
- [15] J. Deng, W. Dong, R. Socher, L.-J. Li, Kai Li, and Li Fei-Fei, “ImageNet: A large-scale hierarchical image database,” in *2009 IEEE Conference on Computer Vision and Pattern Recognition*, 2009, pp. 248–255.
- [16] S. Kullback and R. A. Leibler, “On Information and Sufficiency,” *Ann. Math. Stat.*, vol. 22, no. 1, pp. 79–86, 1951.
- [17] Z. Wang, A. C. Bovik, H. R. Sheikh, and E. P. Simoncelli, “Image quality assessment: from error visibility to structural similarity,” *IEEE Trans. Image Process.*, vol. 13, no. 4, pp. 600–612, Apr. 2004.
- [18] A. Radford, L. Metz, and S. Chintala, “Unsupervised Representation Learning with Deep Convolutional Generative Adversarial Networks,” in *International Conference on Learning Representations*, 2016.
- [19] I. Gulrajani, F. Ahmed, M. Arjovsky, V. Dumoulin, and A. C. Courville, “Improved Training of Wasserstein GANs,” in *Advances in Neural Information Processing Systems 30*, I. Guyon, U. V. Luxburg, S. Bengio, H. Wallach, R. Fergus, S. Vishwanathan, and R. Garnett, Eds. Curran Associates, Inc., 2017, pp. 5767–5777.
- [20] T. Miyato, T. Kataoka, M. Koyama, and Y. Yoshida, “Spectral Normalization for Generative Adversarial Networks,” in *International Conference on Learning Representations*, 2018.
- [21] “scipy.stats.kstest — SciPy v0.14.0 Reference Guide.” [Online]. Available: <https://docs.scipy.org/doc/scipy-0.14.0/reference/generated/scipy.stats.kstest.html>. [Accessed: 06-Nov-2019].
- [22] A. R. Backes, D. Casanova, and O. M. Bruno, “Color texture analysis based on fractal descriptors,” *Pattern Recognit.*, vol. 45, no. 5, pp. 1984–1992, May 2012.
- [23] H. Zhao, O. Gallo, I. Frosio, and J. Kautz, “Loss Functions for Image Restoration With Neural Networks,” *IEEE Trans. Comput. Imaging*, vol. 3, no. 1, pp. 47–57, Mar. 2017.